JOURNAL OF GEOPHYSICAL RESEARCH, VOL. 98, NO. A10, PAGES 17,525–17,535, OCTOBER 1, 1993

FUV-Visible Photometric Imaging of Aurorae

W.K. TOBISKA,[1,2] G.R. GLADSTONE,[1,3] S. CHAKRABARTI,[1,4] M.G. SHEPHERD,[5,6]

J.C. MCCONNELL,[5] R. LINK,[1,3] G. SCHMIDTKE,[7] AND G. STASEK[8]

Photometric images of 130.4-, 337.1-, 391.4-, and 557.7-nm auroral airglow emissions are presented for November 16, 1980, and December 9, 1981. Unique observations and new data reduction techniques allow 360° imaging of the local auroral emissions on both days and a view of spatial and temporal variability. The 1980 aurorae, one nonpulsating and one pulsating, are located in the morning sector. We find that the 1980 diffuse, nonpulsating aurora was located < 75 km from the rocket in a northern location with respect to the rocket and was produced by electrons with a characteristic energy of 200-300 eV. The pulsating aurora was located > 75 km in a western location and was produced by electrons with a characteristic energy of 2-3 keV. Both the near (northern) and far (western) aurorae had motion and size characteristics consistent with northeasterly drift rates of 200-500 m s^{-1} and 30-50 km in size, respectively. The 1981 flight observed a stable arc in the evening sector. The arc was produced by electrons with a characteristic energy of 1-3 keV and had a probable 1/*e* width of approximately 75 km. For both flights, the 557.7/391.4 and 337.1/391.4 ratios were approximately constant.

INTRODUCTION

The flight of the E-2 payload during the Energy Budget Campaign (EBC) in 1980, which included the EF-11 spectometer/photometer, and the reflight of the spectrometer/photometer experiment a year later in 1981 provided detailed information on the spatial, temporal, and spectral characteristics of diffuse and stable arc aurorae, respectively. The EBC, as summarized by *Offermann* [1985], studied the structure and variability of the upper atmosphere due to indirect solar energy inputs. *Seidl et al.* [1983] and *Schmidtke et al.* [1985] describe the two rocket flights and the EF-11 instrument in detail.

Briefly, the EF-11 instrument package consisted of spectrometer and photometer units. Nine detectors scanned wavelength ranges in two spectrometers from 50- to 240-nm with 1-nm resolution and from 105- to 640-nm with 3-nm resolution. Nine additional photometer channels observed discrete emissions from the extreme ultraviolet (EUV) to the visible part of the electromagnetic spectrum. The photometer fields of view for channels 6 through 9 (130.4-, 337.1-, 391.4-, and 557.7-nm, respectively) used in this study were 4°.6 horizontal and 4°.7 vertical (i.e., along the rocket axis) or approximately 9°×10°. The photometer (halfwidth) passband of channel 6 (130.4-nm) was 17.5-nm with < 1% transmission at 121.6-nm, of channel 7 (337.1-nm) was 9.0-nm, of channel 8 (391.4-nm) was 7.8-nm, and of channel 9 (557.7-nm) was 3.7-nm. In both flights, the rockets were stabilized nearly vertically and the instruments sensed horizontally, with the spectrometer and photometer units viewing 180° apart. This instrument configuration, combined with the ~2.5 Hz spin frequency of each rocket, allowed a 360° view as a function of altitude in the auroral region above the launch facilities at Kiruna, Sweden (67.9 N, 21.1 E) for both flights. The first flight was on November 16, 1980 (EBC payload E-2, Salvo B, 0312 UT, hereinafter referred to as flight 1) and the other was on December 9, 1981 (2125 UT, hereinafter referred to as flight 2).

The 20-spin averaged height profiles of the 130.4- 337.1-, 391.4-, and 557.7-nm photometer-measured emissions, the spectrometer observations from 100- to 640-nm for both flights, and a preliminary overview of the data are presented by *Seidl et al.* [1983] and by *Schmidtke et al.* [1985]. Shepherd et al. (unpublished manuscript, 1993) have presented a detailed analysis of the sources of the 557.7-nm emission observed during flight 1. The current work presents a detailed look at the FUV-VIS photometer data along with a preliminary morphological study of temporal and spatial distribution of the observed aurorae of flights 1 and 2.

EF-11 INSTRUMENT DATA REDUCTION

Photometric data for both flights of the EF-11 instrument were processed to provide spatial and temporal information of the auroral features during flight 1 and the stable arc aurora during flight 2. Photometers of the EF-11 instrument recorded the emissions at 83.4-, 98.9-, 120.0-, 168.8-,

[1] EPAG/SSL, Univ. of California, Berkeley, California.

[2] Now at TELOS/JPL, Pasadena, California.

[3] Now at SWRI, San Antonio, Texas.

[4] Now at CSP, Boston Univ., Boston, Massachusetts.

[5] CRESS, York Univ., North York, Ontario, Canada.

[6] Now at Herzberg Institute of Astrophysics, NRCC, Ottawa, Ontario, Canada.

[7] IPM, Freiburg, Germany.

[8] PTS, Freiburg, Germany.

Paper number 92JA02561.
0148-0227/93/92JA-02561$05.00

215.0-, 130.4-, 337.1-, 391.4-, and 557.7-nm at a rate of one data point every 4 ms or about 100 measurements per spin. Photometer data for the first five emissions are not presented here due to low signal-to-noise ratios. A rather unique feature of the experiment was that the rocket spin axis was stabilized in the vertical direction with the instrument field of view perpendicular to the spin axis. This contrasts with the more traditional auroral viewing geometry parallel to the rocket spin axis. The resulting horizontal view of the instrument made possible a spatial mapping of the local auroral emissions over 360° relative azimuth with a time resolution of the rocket spin rate.

The data reduction was complicated as a result of unavailable aspect information for these two flights. The general sequence of data reduction was as follows. The auroral images for both flights 1 and 2 were produced by first binning the data by altitude and then sorting it into relative azimuth angles, each covering 9°. In each altitude layer, which typically covered less than a kilometer, the relative azimuth angle of maximum intensity was shifted such that the maxima were placed at a common azimuth angle. The algorithm was similar for both flights. The results are shown as Plate 1 for flight 1 and Plate 2 for flight 2. The upleg and downleg panels are shown for each of four emissions during both flights and a detailed explanation of the plates occurs below.

Reduction of the data for flight 1 was complicated in part by an apparent change in the rocket spin rate which appeared as a nonstationary periodicity between successive minima in the photometer count rates. In effect, the observed spin rate increased uniformly from 2.5 to 2.7 Hz during flight 1 with smaller magnitude periodic and random spin rate fluctuations superimposed upon the secular change. R. Grabowski (private communication, 1991) has independently confirmed an increasing spin rate of flight 1 attitude data from 2.5 to 2.7 Hz. These nonstationary effects were removed from the data set to obtain auroral images combining temporal and spatial information described below and to provide a view of the local auroral emissions for comparison to ongoing modeling efforts.

Three separate phenomena can account for these apparent spin rate variations. First, the flight 1 rocket [*Offermann*, 1985; *Grabowski et al.*, 1985] moved northward with an average velocity of 160 m s^{-1} over a trajectory groundtrack distance of 72 km during the approximate 450 s of total flight. This rocket motion relative to an Earth reference frame (i.e., parallax) was combined with a radar-measured 200 to 500 m s^{-1} northward electron drift velocity [*Grabowski et al.*, 1985] assumed to be coincident with regional auroral patch motions in an Earth reference frame. These two motions combined to produce a unique observational geometry of the moving auroral patches by the rocket-borne photometers which resulted in only small apparent parallax. To first order, the rocket and aurorae were moving in the same direction with approximately similar velocities. *Swift* [1981] noted that an eastward drift direction is typical of a morning sector diffuse pulsating aurora located equatorward of the auroral emission region. His 100-1000 m s^{-1} range of velocities bracket the *Grabowski et al.* [1985] measurements. In addition, the parallel electron beams from 150 to 230 km at the 166° and 260° angles in the 391.4-nm observations indicate no evidence of significant distance changes between the field lines during the flight. Hence this signifies no strong velocity shears between the patches nor strong electric field gradients [*Johnstone*, 1978]. The deduction is that neither rocket/aurorae relative motion taken alone nor both motions taken together is able to reproduce the observations during the flight without the inclusion of a third component contributing to an apparent spin rate increase. In other words, the parallax effect was not a major contributor to the observed increase in the spin rate of flight 1 although this effect can be seen in flight 2.

Surprisingly, it seems that during flight 1 an actual increase in the spin rate occurred. A rocket spin rate can be increased by applying torque to the vehicle using a force in the proper direction at an appropriate lever arm. In the case of flight 1, the relative angle through which the rocket-to-aurora line-of-sight vector changed was approximately 30° from an initial reference point using the observed auroral features at the start of the flight. The direction of relative angular change of the two auroral patches was consistent with rocket spinup having an angular motion of about 0.08° s^{-1}.

Assuming a Skylark rocket moment of inertia similar to that of a small spinning spacecraft, a thruster force of approximately 0.1 N perpendicular to the spin axis or, equivalently, a pressure of about 1×10^4 Pa at a 0.1 cm^2 vent would be sufficient to produce this spinup. A potential mechanism for this pressure at a vent in the rocket skin is suggested below.

The E2 rocket carried an infrared grating spectrometer [*Offermann*, 1985] in addition to the spectrometers described above. *Grossman et al.* [1981] describe the operation of the infrared instrument which contained a 10 liter liquid helium tank (filled with approximately 1/2 kg of helium (K.U. Grossman, private communication, 1992)). Cooling of the infrared instrument to 4.3 K was obtained by liquid helium evaporation which was subsequently exhausted to a radiation shield near the skin of the rocket. If approximately 10% of the helium was released during the flight (K.U. Grossman, private communication, 1992) with a mass flow of 5×10^{-2} g s^{-1} through vent(s) in the rocket skin totaling 0.1 cm^2, then gas particle exit velocities on the order of 5 m s^{-1} would have produced an exit pressure of 1×10^4 Pa. These are reasonable values for considering helium venting as a candidate to produce the increasing rocket spin rate.

K.U. Grossman (private communication, 1992) noted that the rocket in flight 1 also had an active attitude control system used to keep the rocket vertically stabilized. Thus it is highly probable that the measured increase in the spin rate occurred as a combined result of both the helium venting and an active attitude control system.

This heuristic argument utilizing rocket trajectory, absolute aurora drift, and rocket helium venting/attitude control, accounts for the observational geometry of both aurorae relative to the flight 1 rocket and can satisfy additional physical constraints for the distance to the two auroral features which are discussed below. The flight 2 rocket had a nearly constant spin rate of about 2.8 Hz with a negligible secular increase in spin rate during the course of the flight.

FLIGHT 1 AURORAE CHARACTERISTICS

The images, summarized in Table 1 for both flights, provide a remarkable wealth of information. The important de-

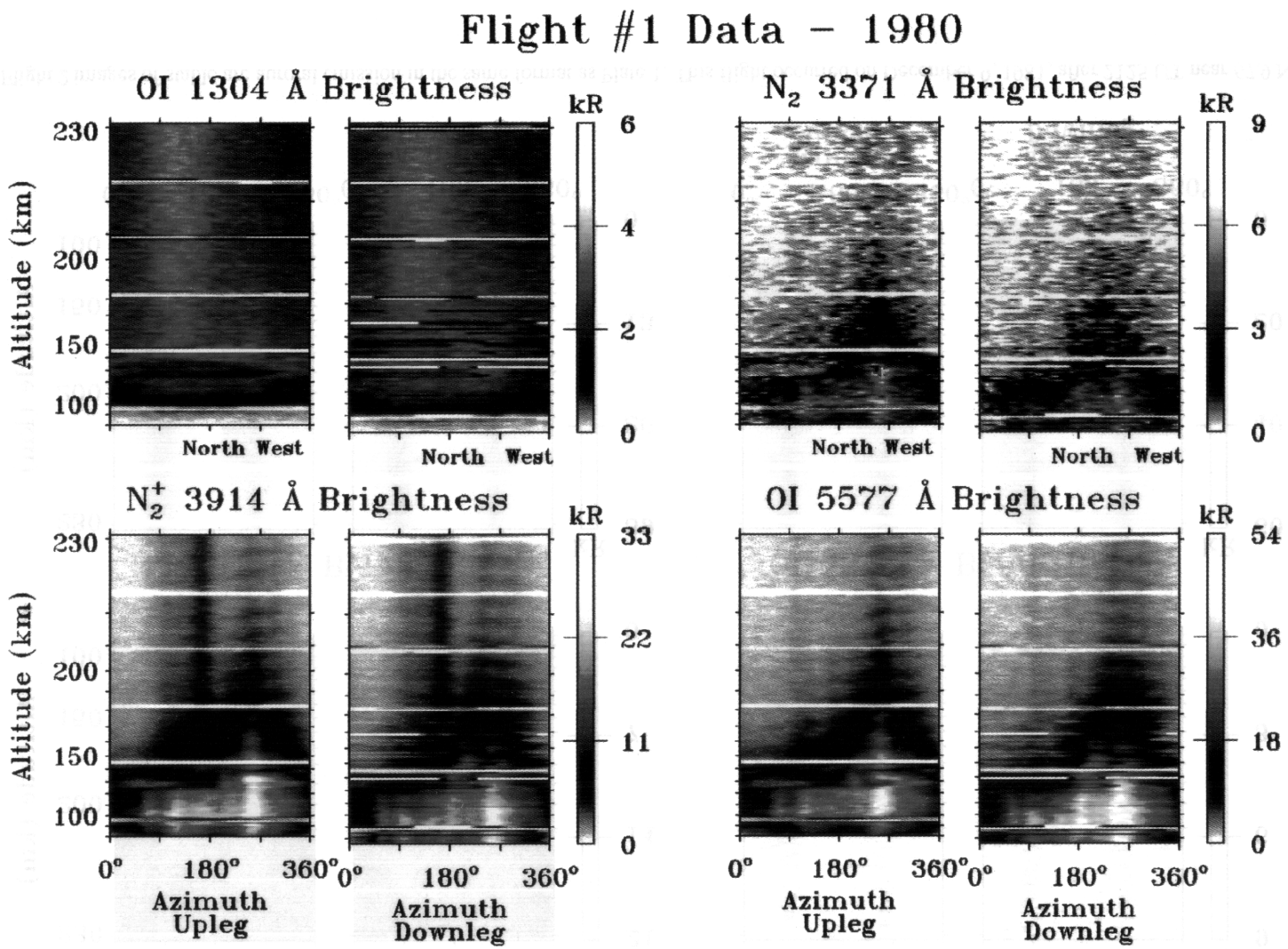

Plate 1. Flight 1 images of diffuse auroral emissions for four emissions observed by 130.4-, 337.1-, 391.4-, and 557.7-nm photometers on the EF-11 instrument during November 16, 1980, after 0312 UT near 67.9 N, 21.1 E. The upleg and downleg flight segments are shown in the left and right panels, respectively. The altitude scale is linear in time while the relative azimuth angle scale covers a 360° view from the rocket from an arbitrary starting position. Emission intensities in kilo-Rayleighs are given by color coding according to the color bar at the right of each set of emissions. White horizontal lines in each panel indicate no data were taken during these altitude (or time) intervals. The abrupt intensity change at 150 km at 166° azimuth in the upleg is a real feature probably due to dynamics but not analyzed in this study.

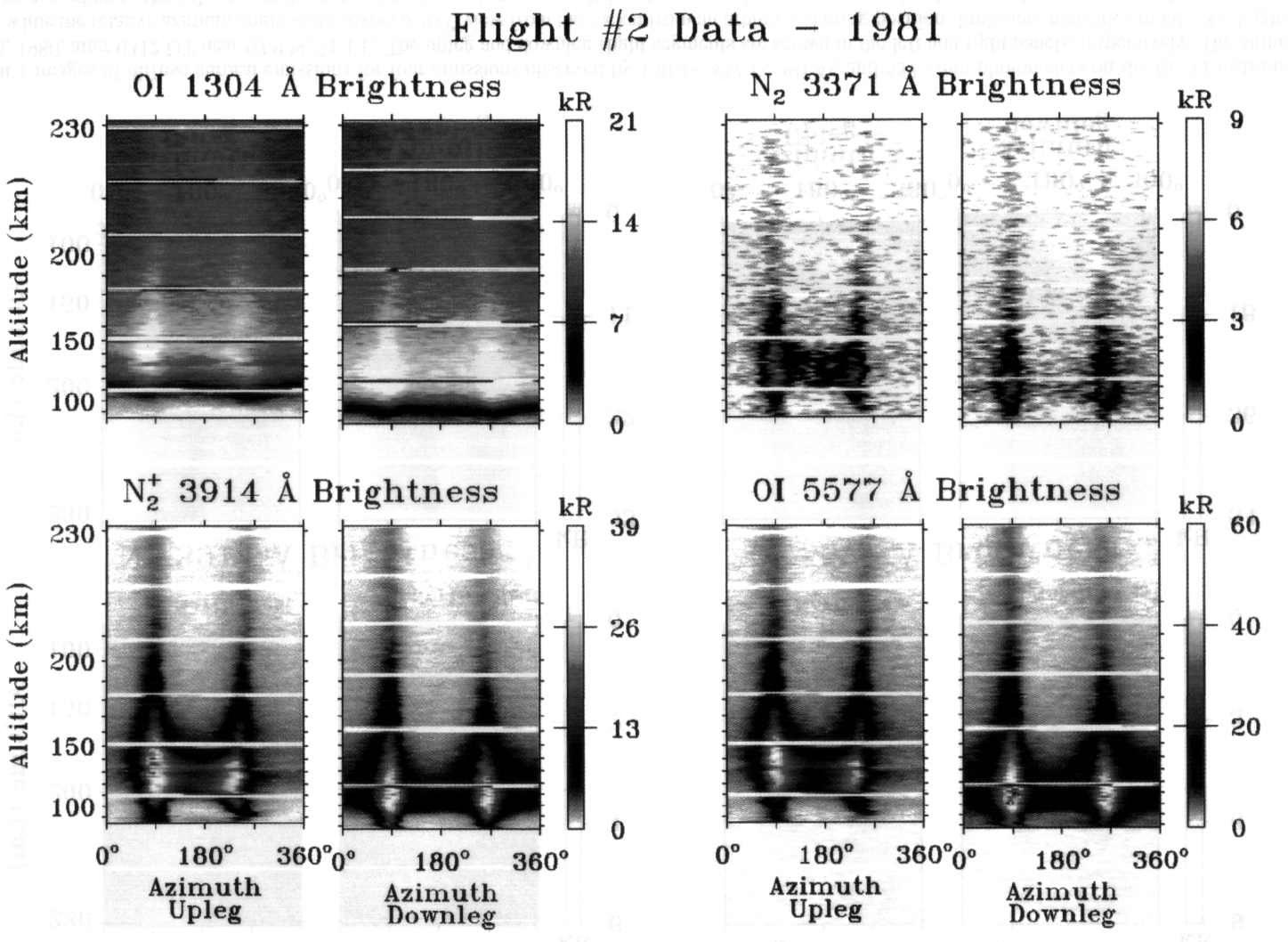

Plate 2. Flight 2 images of stable arc auroral emission in the same format as Plate 1. This flight occurred on December 9, 1981, after 2125 UT near 67.9 N, 21.1 E.

TABLE 1. EF-11 FUV-VISIBLE AURORAE CHARACTERISTICS

	Flight 1 November 16, 1980 U.T. 0312	Flight 1 November 16, 1980 U.T. 0312	Flight 2 December 9, 1981 U.T. 2125
Auroral features	nonpulsating diffuse early morning sector northward drift	pulsating diffuse early morning sector 13 s period 8±2 s duration northward drift	nonpulsating arc evening sector stable, no drift
Relative azimuth angle (brightest emissions)	120° [a], 166° [b]	260° [b]	90° — 180°
Distance to aurora	< 75 km	> 75 km	60 [f] — 10 [g] km
Aurora location [c]	north	west	east — west (curtain)
Primary electron characteristic energy	200 — 300 eV	100 — 500 [d] eV 2 — 3 [e] keV	0.9 [f] keV to 2 — 3 [g] keV
Peak emission intensity of polynomial fit [j]			
130.4	3 [f g]	2 [f g]	14 — 17 [f g h], 13 — 17 [f g i]
337.1	3 [f g]	5 [f], 3 [g]	4 [f h], 3 [f i], 3 [g h i]
391.4 [d]	2 [f g]	—	—
391.4 [e]	16 [f g]	23 [f g]	25 [f g h], 23 [f g i]
557.7	26 [f], 32 [g]	35 [f], 41 [g]	35 — 36 [f g h], 29 [f i], 40 [g i]
Peak emission altitude of polynomial fit [k]			
130.4	≥ 210 [f], > 190 [g]	≥ 140 [f], ≥ 210 [g]	155 [f h i], 124 [g h i]
337.1	106 [f g]	96 [f], 103 [g]	121 [f h], 117 [f i], 108 [g h i]
391.4 [d]	≥167 [f], ≥177 [g]	—	—
391.4 [e]	101 [f g]	108 [f], 103 [g]	126 [f h], 119 [f i], 107 [g h i]
557.7	110 [f g]	113 [f], 105 [g]	132 [f h], 123 [f i], 108 [g h i]

Both flights launched from Kiruna, Sweden (67.9 N, 21.1 E).
[a] Optically thick emission only (OI 130.4).
[b] Optically thin emission only (N_2 337.1, N_2^+ 391.4, O 557.7).
[c] Relative to the rocket in an Earth-centered reference frame.
[d] Softer electron population (with pronounced pulsations).
[e] Harder electron population (with ambiguous pulsations).
[f] Upleg.
[g] Downleg.
[h] Easterly arc segment.
[i] Westerly arc segment.
[j] In kilo-Rayleighs; a quartic polynomial fit through the data at the relative azimuth angle of maximum peak emission produced this value.
[k] In kilometers; a quartic polynomial fit through the data at the relative azimuth angle of maximum peak emission produced this value.

tails of Table 1 are discussed in this and the following section.

For flight 1, Plate 1 shows images of auroral emissions apparently excited by two separate streams of precipitating electrons. For each of four emissions, 130.4-, 337.1-, 391.4-, and 557.7-nm, the upleg and downleg flight segments are shown in the left and right panels, respectively. The altitude scale is linear in time while the relative azimuth angle scale covers a 360° view from the rocket from an arbitrary starting position. Emission intensities in kilo-Rayleighs are given by color according to the color bar at the right of each set of emissions. White horizontal lines in each panel indicate no data were taken during these altitude (or time) intervals. Major features common to all panels are the vertical columns of emission up to 230 km at particular azimuth angles, the "pulsating" features in the 337.1-, 391.4-, and 557.7-nm emissions between 150 and 230 km near 260° relative azimuth angle, and the peak intensities between 100 and 140 km altitude for these three emissions. Each pulsation segment on the upleg has a small positive slope

suggesting a change in intensity over a small altitude increment. This is a data processing artifact resulting from sampling a specific azimuth location combined with the coarseness of the altitudinal binning. The small negative slope in each pulsation on the downleg, compared to the upleg, is also an artifact of the image display process. The continuous data set for the flight is split into upleg and downleg segments and the downleg data array is reversed to portray the emissions for the same altitudes as the upleg. In the 391.4-nm panels, the presence of two distinct aurorae was not suspected in earlier analyses [*Seidl et al.*, 1983; *Schmidtke et al.*, 1985].

Characteristics of two assumed streams of electron precipitation during flight 1 are as follows. The observed 391.4-nm emissions, which result from electron impact ionization of N_2 and are optically thin, occur along the field lines above 90 km at the 166° and 260° relative azimuth angles. Pulsations were initially noted by *Schmidtke et al.* [1985] in the preliminary analysis of the 391.4/557.7 emissions and were also suggested by measurements of variable electron fluxes on the same rocket flight [*Torkar et al.*, 1985]. Detailed analysis in this study indicates that pulsations are clearly evident from 150 km to 230 km altitude in the 391.4- and 557.7-nm observations at the 260° angle during both the upleg and downleg flight segments and are slightly visible at the 166° angle.

In the pulsating aurora, the pulsation rate is almost constant through the flight at approximately 13 s with a duration of about 8±2 s per pulse. Time resolution of the data was not sufficient to determine the length of time for pulse turn on and off. The relative amplitude of the pulses compared to the mean background level at each altitude layer is ±20% with the background ranging from 15-3 kilo-Rayleighs for the 391.4-nm emission (150-230 km, respectively). The relative amplitude increases with decreasing altitude in these observations. This is consistent with observations of pulsating patchy aurorae in the morning sector as reviewed by *Paulson and Shepherd* [1966], *Pemberton and Shepherd* [1975], *Davis* [1978], and *Johnstone* [1978] and as described in detail by *Røyrvik and Davis* [1977] and *Swift* [1981]. Figure 1 shows this information with the averaged flight 1 391.4-nm emission upleg pulsating profile centered at 263±23° relative azimuth angle, the normalized residuals produced by the subtraction of the mean background from the upleg data expressed as a percentage change, and the normalized power spectrum.

No pulsations or enhanced emissions at the 260° angle are evident in the OI 130.4-nm image. This is interpreted as evidence that the pulsating aurora at 260° relative azimuth angle is > 75 km away (greater than an O scale height) so that 130.4-nm emissions are extinguished by resonance scattering before reaching the rocket. Fourier analysis of the 337.1-nm emission shows evidence of pulsation at the 260° angle although the data is much noisier. These pulse observations are different from *Torkar et al.* [1985], who report in situ 5 s characteristic duration pulses for electrons with energies > 16.3 keV having pitch angles between 20° and 45° on the same flight. The longer pulse period remotely observed in the optical emissions is probably due to the generation of visible emissions by electrons on more distant field lines.

The energy of the precipitating electrons in flight 1 can be generally determined from a combination of factors. First,

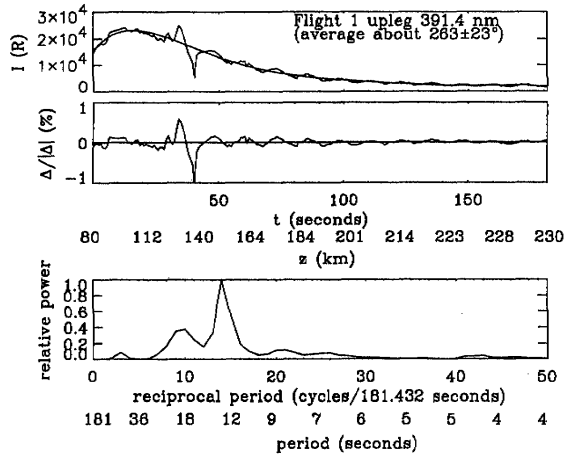

Fig. 1. Flight 1 averaged upleg 391.4-nm emission showing the pulsating profile centered at 263±23° relative azimuth angle (top panel with abscissa linear in time). The middle panel, also linear in time, shows the normalized residuals produced by the subtraction of the mean background from the upleg data expressed as a percentage change. The normalized power spectrum is shown in the bottom panel for the profile and indicates that there is a pulse period of about 13 s.

the range of primary electron energy is bracketed by the cross section of N_2^+ 1N (see Figure 2) where the 391.4-nm emissions are produced by electrons ranging from 20 eV to greater than 10 keV. The N_2 2P 337.1-nm emission is produced by softer energy secondary electrons in the range of 10-40 eV. The 337.1- and 557.7-nm emissions are apparent at the 260° angle, along with the 391.4-nm emission, while they are much weaker at the 166° angle. Thus along the 260° azimuth angle electron stream there is a strong argument for an electron flux containing harder characteristic energy electrons which would produce a substantial quantity of secondary electrons. The N_2 was subsequently ex-

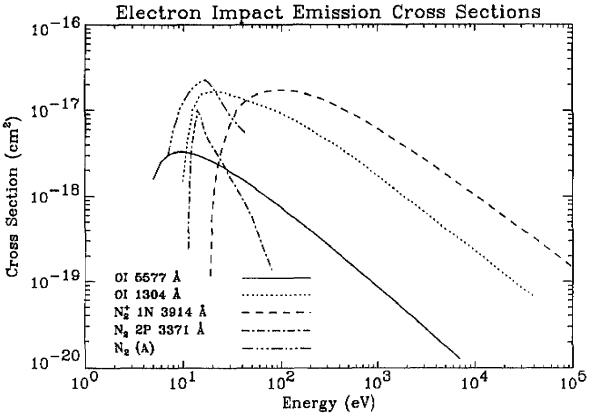

Fig. 2. Electron impact emission cross sections plotted by electron energy in eV for emissions observed in flights 1 and 2. The OI 557.7-nm cross section is given by *Jackman et al.* [1977], OI 130.4-nm by *Zipf and Erdman* [1985], N_2^+ 1N 391.4-nm by *Borst and Zipf* [1970], and $N_2$2P 337.1-nm as well as N_2(A) by *Cartwright et al.* [1977].

cited by these secondaries to produce the 337.1-nm emission and the $N_2(A)$ state which then produces most of the OI 557.7-nm emission (Shepherd et al., unpublished manuscript, 1993). The presence of more energetic electrons are thus consistent with observations of the N_2^+ 391.4-, N_2 337.1-, and OI 557.7-nm emissions along the 260° angle. Next, an upper energy limit is suggested from the pulsation rate where 10 keV auroral electrons have a bounce period of about 4 s in a closed field [*Paulson and Shepherd*, 1966; *Johnstone*, 1978] implying that the 13 s period electrons in the pulsating aurora at 260° angle have a characteristic energy of less than 10 keV. Finally, the observed altitude of the 23-kilo-Rayleighs peak 391.4-nm upleg emission at the 260° angle is 108 km which corresponds to a characteristic electron energy of 2-3 keV with a Maxwellian distribution [*Strickland et al.*, 1989]. The 103-km intensity peak in the downleg 337.1-nm corresponds to Maxwellian electron spectra with a characteristic energy of about 4 keV [*Daniell and Strickland*, 1986] which is consistent with the 391.4-nm observations. These deductions support *Torkar et al.* [1985], who found the average in situ measured integral energy flux of 0.1-25 keV electrons along the trajectory to be 0.4 ergs cm^{-2} s^{-1} sr^{-1} with the largest number of primaries in the 1.2-5.8 keV range.

Along the 166° angle there are negligible 337.1- and 557.7-nm emissions compared with the large intensities in 391.4-nm above 150 km. The explanation for this is an unresolved challenge in evaluating the flight 1 data sets. If production of secondary electrons is independent of primary energy, then a softer aurora should not affect the presence of the 557.7- and 337.1-nm emission. There is evidence of a softer aurora at the 166° relative azimuth angle in both upleg and downleg segments as shown in Figure 3 (upleg) where the low energy electron component of the 391.4-nm emission is recovered by subtracting the 557.7-nm emission normalized to the 391.4-nm values. The soft aurora begins to fall off sharply below 167 km, suggesting a characteristic energy of about 200-300 eV for the electrons in this assumed electron stream [*Strickland et al.*, 1989] with a 391.4-nm intensity of 2-3 kilo-Rayleighs.

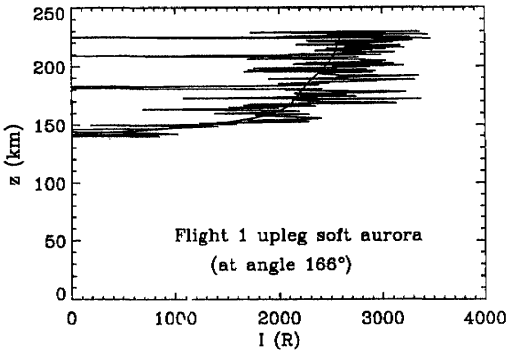

Fig. 3. The low energy electron component of the 391.4-nm emission in Flight 1 upleg data at the 166° relative azimuth angle is plotted by intensity and altitude. This profile is recovered by subtracting the 557.7-nm emission normalized to the 391.4-nm values. The smooth line through the data is a quartic polynomial fit to give the reader a general sense of the intensity profile (cf. Table 1, note k).

Table 1 summarizes additional details of the other emissions at this relative azimuth angle. If the atomic oxygen is wholly depleted or there is a sunlit aurora, then 557.7-nm emission may not be present. Oxygen is not completely depleted, as evidenced by the 130.4-nm emission, and the time of flight occurred in near darkness when the sun was approximately 23° below the horizon. The broad nonpulsating OI 130.4-nm emissions centered at an azimuth angle of about 120° may be due to resonantly scattered sunlight around the terminator from the dayside, or it could be a results of a soft aurora. Likewise, it is possible that scattered sunlight may contribute to the nonpulsating 391.4-nm emission at 166°, although the large solar declination makes this seem unlikely. More detailed modeling is required to help resolve these questions.

The brightness ratios of the OI 557.7- to N_2^+ 391.4-nm and N_2 337.1- to N_2^+ 391.4-nm emissions are shown in Plate 3 for both flight 1 and 2 upleg and downleg observations. In flight 1, the 557.7/391.4 ratio is nearly constant for both the 260° angle aurora (1.8 above 150 km) produced by higher energy electrons and the 166° angle aurora (about 1). The sharp ratio change below 150 km at the 166° angle suggests an emission produced by more energetic electrons similar to the 260° angle aurora. Without aspect information for this flight, it is not possible to determine if the lower altitude emission is physically associated with the farther aurora. There is weak evidence of pulsations in the 557.7-nm emission near the 166° angle above 150 km although there is no evidence of pulsations in the softer aurora shown in Figure 3. Thus 391.4-nm emission at the 166° angle may contain information from two separate auroral sources, one pulsating and clearly evident at altitudes below 150 km and one nonpulsating above 150 km.

The ratio of the 337.1/391.4-nm emissions at 260° was nearly constant for both the upleg and downleg observations as shown in Plate 3. This supports the conclusions of *Strickland et al.* [1989], *Solomon* [1989], *Richards and Torr* [1990], and *Gattinger et al.* [1991], who show modeling and experimental results indicating secondary production rates are independent of the primary characteristic energy when the latter are greater than 1-2 keV. However, this contradicts results of *Rees and Lummerzheim* [1989], who find a secondary dependence on primary energies. M.H. Rees (private communication, 1991) indicates that recent changes in the Rees and Lummerzheim model have removed this secondary dependence. Figure 4 shows the upleg and downleg ratios for both flights at greater resolution than Plate 3 for the 260° relative azimuth angle. In flight 1 (top panel), the 0.16 mean value for all altitudes is lower than *Sharp et al.* [1979] and *Gattinger et al.* [1991], who have found this ratio to be nearer 0.25-0.30. The discrepancy of the ratio magnitude, which is a factor of 2 lower than previous observations, is still being investigated and may be due to poor signal-to-noise ratio or calibration uncertainty in the 337.1-nm photometer. One notes in Plate 3 and Figure 4 that, for higher count rates at lower altitudes, the ratio approaches the 0.25 value. The spread of the ratios in Figure 4 can be attributed to low count rates for 337.1-nm measurements.

For flight 1, the distance from the rocket to the aurora can be estimated from the optically thick 130.4-nm emission. Assuming that emission at the 166° angle is due to a soft aurora, it must be closer than about one atomic oxygen

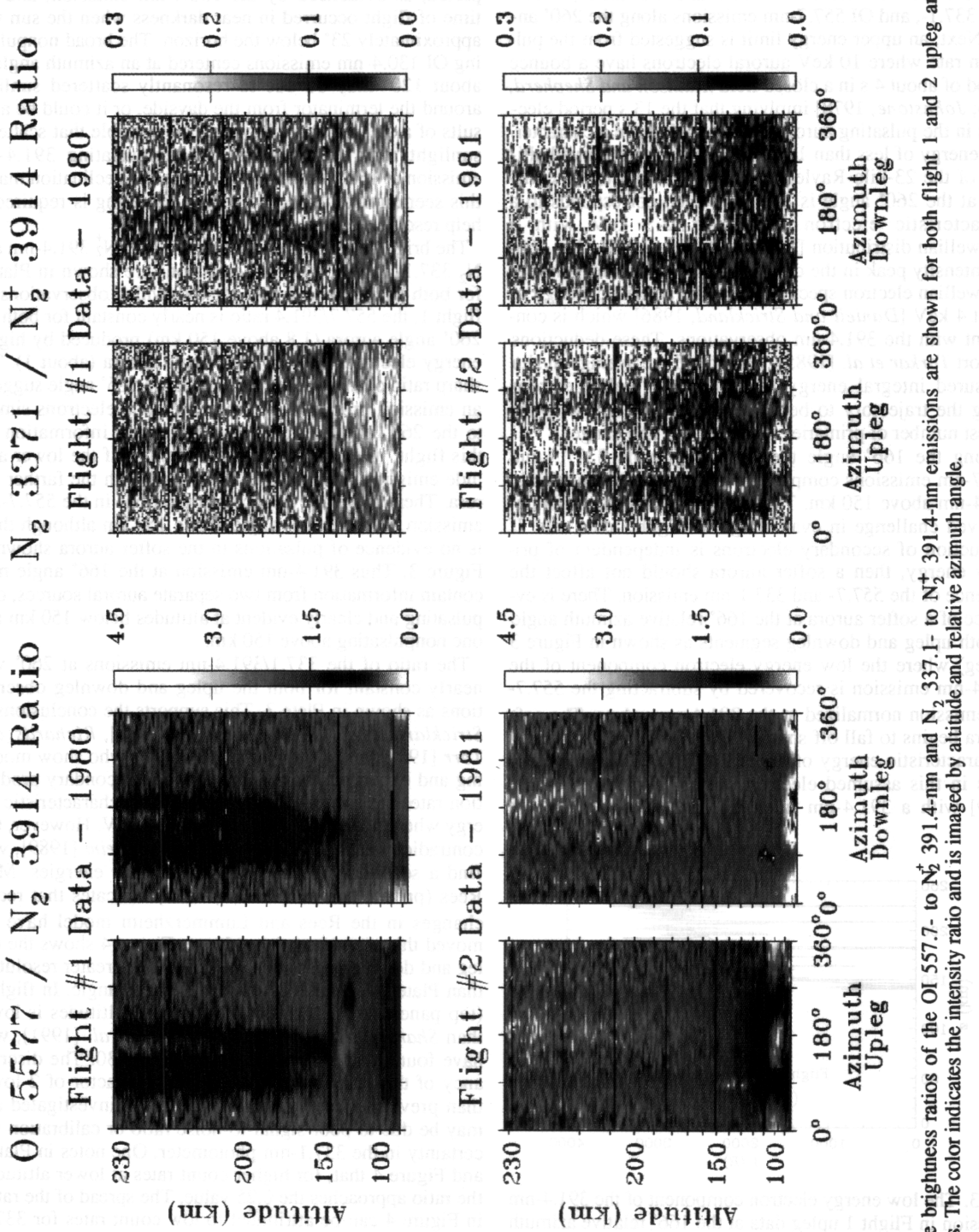

Plate 3. The brightness ratios of the OI 557.7- to N_2^+ 391.4-nm and N_2 337.1- to N_2^+ 391.4-nm emissions are shown for both flight 1 and 2 upleg and downleg observations. The color indicates the intensity ratio and is imaged by altitude and relative azimuth angle.

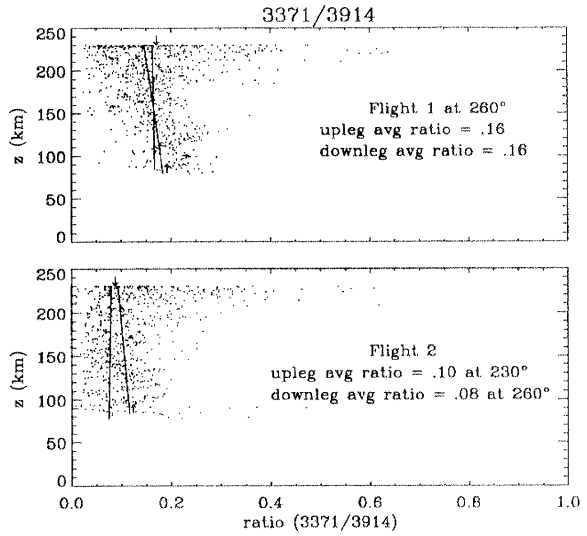

Fig. 4. The upleg and downleg average 337.1/391.4 ratios for the 260° relative azimuth angle (Flight 1) and the 230° relative azimuth angle (Flight 2) are shown. The linear fit to the ratios, derived by fitting the ratio data to the independent altitude data, are plotted by altitude and are shown with up and down arrows to the right of each line.

scale height (i.e., ~75 km) to be visible in the 130.4-nm emission from 230 to 130 km altitude. From the absence of the 130.4-nm emission, it can be deduced that the auroral patch at the 260° angle is farther than ~75 km away, depending on the size of the patch, since the expected emission of ~20-30 kilo-Rayleighs is extinguished by resonance scattering down to 1-2 kilo-Rayleighs at all altitudes.

The size of the auroral patch in flight 1 above 150 km can also be estimated. The brightest 391.4-nm emission at the 166° angle spanned about 12° in 1/*e* width (from peak intensity to 1/*e* of peak) of relative azimuthal angle as viewed from the rocket location. This suggests an auroral 1/*e* width above 150 km altitude on the order of 30 km, if the feature is not due to scattered sunlight. By the same argument, the pulsating aurora at the 260° angle, with a 1/*e* width of 13°, would then be on the order of 50 km in 1/*e* width which agrees with previous observations of pulsating auroral patches between 50 and 100 km in width [*Johnstone*, 1978; *Swift*, 1981].

In summary, the geometry of the aurora from flight 1 using these observations and deductions can be illustrated in Figure 5 where the rocket trajectory groundpath and both aurorae locations are shown. The farther, pulsating aurora is the one located to the west of the rocket trajectory while the nearer, diffuse aurora is generally to the north of the trajectory.

FLIGHT 2 AURORA CHARACTERISTICS

Flight 2 images in Plate 2 reveal an evening sector stable auroral arc with a constant flux of precipitating electrons. The format of Plate 2 is the same as Plate 1 discussed above. For all four photometers, columns of emission between 100 and 230 km are seen at the same relative azimuth angles of 90 and 270°. This is consistent with a rocket flying outside of and into a stable arc. All four emissions exist coincident with one another and there were no apparent pulsations.

During flight 2, the altitude of peak emission moved downwards by about 18 km from 126 to 108 km during the flight suggesting a hardening of the characteristic energy of the electrons. This hardening is probably related to the position of the rocket with respect to the aurora (i.e., on the edge during upleg, in the middle during downleg). From *Strickland et al.* [1989] these altitudes of maximum 391.4-nm emission correspond to approximately 1-3 keV characteristic electron energies from the upleg to the downleg, respectively. The 391.4-nm emissions at the 90° relative azimuth angle were approximately the same for both legs of the flight at 30 kilo-Rayleighs. The 391.4-nm emission at the 270° relative azimuth angle was slightly less at about 25 kilo-Rayleighs. Table 1 summarizes the intensity and altitude details of the other emissions.

Flight 2 showed no significant change in the average number of measurements per spin, unlike flight 1. The observed width of the stable arc is quite clearly defined in all photometer observations, covering about 15° to 20° in 1/*e* width for relative azimuthal angles. A parallax effect was observed between the upleg and downleg in all emissions where an example is the relative angle of separation between peak emissions in the 130.4-nm data ranging from 162° to 185° from the beginning to the end of flight. This suggests the upleg was generally to one side of the arc while the downleg was generally in the middle of the aurora. Preliminary modeling of the optically thin 391.4-nm emission, using a groundtrack distance of 50 km between the peak observations from the upleg to the downleg, suggests that a 600-km-long stable arc with a 1/*e* width of 75 km (center of arc to 1/*e* point) provides the shape and intensity observed in the 391.4-nm feature. This is consistent with an observed 1/*e* width of 19° in relative azimuth angle. Preliminary modeling of the optically thick OI 130.4-nm emission using the two-dimensional radiative transfer code of *Gladstone* [1992] suggests that the 130.4-nm emissions should be relatively constant with azimuth angle, and that the observed brightenings at the 90° and 270° angles are

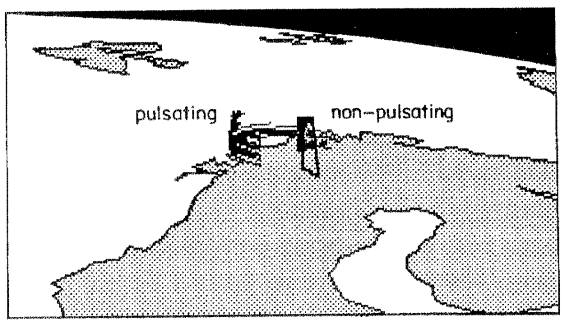

Fig. 5. The geometry of the aurora from flight 1 using the observations and deductions in the text are illustrated where the rocket trajectory, groundpath, and both aurorae locations are shown. The pulsating aurora is located to the west of the rocket trajectory > 75 km (arbitrarily set to 200 km here) while the nonpulsating diffuse aurora is generally to the north of the trajectory < 75 km (arbitrarily set to 50 km here).

likely due to contamination from the nearby optically thin OI 135.6-nm emission and possibly N_2 LBH emissions as well.

The 391.4/557.7 ratio is independent of altitude above 150 km [*Schmidtke et al.*, 1985]. Plate 3 shows the nearly constant ratio of the OI 557.7- to N_2^+ 391.4-nm emissions (near 2) for both legs of the flight. The ratio discrepancy on the bottomside of the upleg (below 120 km) is likely a result of increased quenching of $N_2(A)$, causing the emission rate of OI 557.7-nm to decrease. The differences between the 391.4-nm and 557.7-nm emissions discussed for flight 1 are not evident in this aurora which is consistent with a single arc produced by common characteristic energy electrons along its length. Scattered sunlight was not a factor in creating these emissions.

The 337.1/391.4 ratio was also constant during the flight as shown in both Plate 3 and Figure 4. The ratio magnitude (0.1) was even lower in this data set, compared to Flight 1 and previous observations, by up to a factor of 3, and again points to the problem of the 337.1-nm low count rate.

CONCLUSIONS

Observations of FUV-VIS aurorae at the 130.4-, 337.1-, 391.4- and 557.7-nm emissions by photometers on two vertically spin-stabilized rockets viewing horizontally (i.e., perpendicular to the spin axis) are described for the auroral region near Kiruna, Sweden. This viewing geometry, combined with unique data reduction techniques, provided spatial imaging of the aurorae over 360° with a time resolution on the order of 1 s for two flights of the same instrument about a year apart. The geometry of the rocket and instrument observations, when combined with the present imaging and data reductions techniques, provide an excellent way to study auroral structure by remote sensing of FUV, UV, and visible emissions. We suggest that this technique be used again, where the availability of aspect information would make the results even more useful. These images are ideal for further model comparisons.

The first flight of the EBC EF-11 instrument package in 1980 observed two separate aurorae in the early morning sector. One interpretation is that a possible precipitating electron stream closer than 75 km to the north of the rocket trajectory (at the 166° relative azimuth angle) contained characteristic energies of 200-300 eV and produced an intensity of 2-3 kilo-Rayleighs in the 391.4-nm N_2^+ emission above 160 km altitude. A second suggestion is that scattered sunlight produced the aurora at the 166° relative azimuth angle. It remains unexplained why there are strong, nonpulsating 130.4- and 391.4-nm emissions at this location and weak, pulsating 337.1- and 557.7-nm emissions in the same general vicinity.

A second stream of precipitating pulsating electrons further than 75 km to the west of the trajectory (at the 260° relative azimuth angle) contained an electron population with higher characteristic energies of 2-3 keV producing an intensity of 23 kilo-Rayleighs in the 391.4-nm upleg emission which peaked near 108 km altitude. This westerly second stream produced an intensity of 3-15 kilo-Rayleighs in the 391.4-nm emission above 150 km. An interesting feature of the pulsating electron population was its pulse period of about 13 s while each pulse had a duration of about 8±2 s. This westerly electron stream produced secondaries which excited the N_2 337.1-nm emission, the latter showing an identical pulse modulation at much weaker intensities.

The 557.7/391.4 and 337.1/391.4 ratios were constant (1.8 and 0.16, respectively) for this flight, especially above 150 km, although the low magnitude of the 337.1/391.4 ratio compared to other experiments reflects large uncertainty such as from low count rates. Assuming nonsunlit aurora, both the near (northern) and far (western) aurorae had motion and size characteristics consistent with northeasterly drift rates of 200-500 m s^{-1} and 30-50 km in size, respectively.

The second flight of the EF-11 instrument package in 1981 observed a stable arc aurora in the evening sector, starting from less than 75 km from the middle of the aurora and ending within the thin, stable arc. Parallax was observed in the upleg and downleg angular separation of the maximum intensities. During this flight, the electron characteristic energy of 1-3 keV appeared to harden as a result of the rocket entering the aurora from the side. The altitude of peak 391.4-nm emission lowered from 126 to 108 km between the beginning and the end of the flight. The maximum intensity of the emission remained relatively constant during the second flight at 25-30 kilo-Rayleighs for the 391.4-nm emission. Preliminary modeling of this emission, to be detailed in a subsequent paper, indicates an arc $1/e$ width of 75 km. The 557.7/391.4 and 337.1/391.4 ratios were generally constant with values near 2 and 0.1, respectively.

Acknowledgments. This work was sponsored by NSF grants ATM-8900145 and ATM-9016975. We thank G. Witt and P. Espy for helpful comments.

The Editor thanks D.P. Steele and another referee for their assistance in evaluating this paper.

REFERENCES

Borst, W. L., and E. C. Zipf, Cross section for electron-impact excitation of the (0,0) first negative band of N_2^+ from threshold to 3 keV, *Phys. Rev. A, 1*, 834, 1970.

Cartwright, D. C., S. Trajmar, A. Chutjian, and W. Williams, Electron impact excitation of the electronic states of N_2. II. Integral cross sections at incident energies from 10 to 50 eV, *Phys. Rev. A, 16*, 1041, 1977.

Daniell, Jr., R. E., and D. J. Strickland, Dependence of auroral middle UV emissions on the incident electron spectrum and neutral atmosphere, *J. Geophys. Res., 91*, 321, 1986.

Davis, T. N., Observed characteristics of auroral forms, *Space Sci. Rev., 22*, 77, 1978.

Gattinger, R. L., A. V. Jones, J. H. Hecht, D. J. Strickland, and J. Kelly, Comparison of ground-based optical observations of N_2 second positive to N_2^+ first negative emission ratios with electron precipitation energies inferred from the Sondre Stromfjord radar, *J. Geophys. Res., 96*, 11341, 1991.

Gladstone, G. R., Auroral resonance line radiative transfer, *J. Geophys. Res., 97*, 1377, 1992.

Grabowski, R., C. Hanuise, E. Nielsen, J. P. Villain, and H. Wolf, Simultaneous measurements of the ionospheric electric field by probes and radar methods, *J. Atmos. Terr. Phys., 47*, 41, 1985.

Grossman, K. U., W. G. Frings, R. Hennig, and D. Offermann, A liquid helium cooled twin grating spectrometer for measurements of upper atmosphere infrared emissions, *Energy Budget Campaign 1980: Experiment Summary*, edited by D. Offermann and E. V. Thrane, p. 256, BMFT-FB-W 81-052, Bundesministerium für Forschung und Technologie, Bonn, 1981.

Jackman, C. H., R. H. Garvey, and A. E. S. Green, Electron impact on atmospheric gases, 1. Updated cross sections, *J. Geophys. Res., 82*, 5081, 1977.

Johnstone, A. D., Pulsating aurora, *Nature, 274*, 119, 1978.

Offermann, D., The Energy Budget Campaign 1980: Introductory review, *J. Atmos. Terr. Phys., 47*, 1, 1985.

Paulson, K. V., and G. G. Shepherd, Fluctuations in brightness from quiet-form auroras, *Can. J. Phys., 44*, 837, 1966.

Pemberton, E. V., and G. G. Shepherd, Spatial characteristics of auroral brightness fluctuation spectra, *Can. J. Phys., 53*, 504, 1975.

Richards, P. G., and D. G. Torr, Auroral modeling of the 3371 Å emission rate: Dependence on characteristic electron energy, *J. Geophys. Res., 95*, 10337, 1990.

Rees, M. H., and D. Lummerzheim, Characteristics of auroral electron precipitation derived from optical spectroscopy, *J. Geophys. Res., 94*, 6799, 1989.

Røyrvik, Ø., and T. N. Davis, Pulsating aurora: Local and global morphology, *J. Geophys. Res., 82*, 4720, 1977.

Schmidtke, G., G. Stasek, C. Wita, P. Seidl, and K. D. Baker, Rocket-borne EUV-visible emission measurements, *J. Atmos. Terr. Phys., 47*, 147, 1985.

Seidl, P., G. Stasek, C. Wita, and G. Schmidtke, Rocket-borne measurements in the EUV-Visible spectral range during auroral events, Proceedings, Sixth ESA Symposium on European rocket and balloon programmes and related research, Interlaken, Switzerland, *Eur. Space Agency Spec. Publ., SP-183*, 77, 1983.

Sharp, W. E., M. H. Rees, and A. I. Stewart, Coordinated rocket and satellite measurements of an auroral event 2. The rocket observations and analysis, *J. Geophys. Res., 84*, 1977, 1979.

Solomon, S. C., Auroral Excitation of the N_2 2P(0,0) and VK(0,9) bands, *J. Geophys. Res., 94*, 17215, 1989.

Strickland, D. J., R. R. Meier, J. H. Hecht, and A. B. Christensen, Deducing composition and incident electron spectra from ground-based auroral optical measurements: Theory and model results, *J. Geophys. Res., 94*, 13527, 1989.

Swift, D. W., Mechanisms for auroral precipitation: A review, *Rev. Geophys. Space Phys., 19*, 185, 1981.

Torkar, K. M., A. Urban, J. Bjordal, J. Å. Lundblad, F. Sørass, L. G. Smith, A. Dumbs, B. Grandal, J. C. Ulwick, and R. P. Vancour, Energy deposition rates by charged particles, *J. Atmos. Terr. Phys., 47*, 61, 1985.

Zipf, E. C., and P. W. Erdman, Electron impact excitation of atomic oxygen: Revised cross sections, *J. Geophys. Res., 90*, 11087, 1985.

S. Chakrabarti, Center for Space Physics, 725 Commonwealth Ave., Boston University, Boston, MA 02215.

G. R. Gladstone and R. Link, Southwest Research Institute, 6220 Culebra Rd., San Antonio, TX 78228.

J. C. McConnell, CRESS, York University, North York, Ontario, Canada M3J 1P3.

G. Schmidtke, IPM, Heidenhofstrasse 8, D-7800 Freiburg, Germany.

M. G. Shepherd, Herzberg Institute of Astrophysics, NRCC, 100 Sussex Dr., Ottawa, Ontario, Canada K1N 0R6.

G. Stasek, PTS, Leinenweberstrasse 16, D-7800 Freiburg, Germany.

W. K. Tobiska, Telos/JPL, MS 264-765, 4800 Oak Grove Dr., Pasadena, CA 91109.

(Received February 10, 1992;
revised October 23, 1992;
accepted October 23, 1992.)